

Enzymatic modification by point mutation and functional analysis of an omega-6 fatty acid desaturase from Arctic *Chlamydomonas* sp.

Woongsic Jung, Eun Jae Kim, Se Jong Han, Sung-Ho Kang, Han-Gu Choi & Sanghee Kim

To cite this article: Woongsic Jung, Eun Jae Kim, Se Jong Han, Sung-Ho Kang, Han-Gu Choi & Sanghee Kim (2017) Enzymatic modification by point mutation and functional analysis of an omega-6 fatty acid desaturase from Arctic *Chlamydomonas* sp., *Preparative Biochemistry and Biotechnology*, 47:2, 143-150, DOI: [10.1080/10826068.2016.1188311](https://doi.org/10.1080/10826068.2016.1188311)

To link to this article: <http://dx.doi.org/10.1080/10826068.2016.1188311>

 View supplementary material [↗](#)

 Accepted author version posted online: 18 May 2016.
Published online: 18 May 2016.

 Submit your article to this journal [↗](#)

 Article views: 28

 View related articles [↗](#)

 View Crossmark data [↗](#)

Enzymatic modification by point mutation and functional analysis of an omega-6 fatty acid desaturase from Arctic *Chlamydomonas* sp.

Woongsic Jung^{a,*}, Eun Jae Kim^{a,b,*}, Se Jong Han^{a,b}, Sung-Ho Kang^c, Han-Gu Choi^a, and Sanghee Kim^a

^aDivision of Polar Life Sciences, Korea Polar Research Institute, Korea Institute of Ocean Science and Technology, Incheon, Republic of Korea;

^bDepartment of Polar Life Sciences, University of Science and Technology, Incheon, Republic of Korea; ^cDivision of Polar Ocean Sciences, Korea Polar Research Institute, Korea Institute of Ocean Science and Technology, Incheon, Republic of Korea

ABSTRACT

Arctic *Chlamydomonas* sp. is a dominant microalgal strain in cold or frozen freshwater in the Arctic region. The full-length open reading frame of the omega-6 fatty acid desaturase gene (AChFAD6) was obtained from the transcriptomic database of Arctic *Chlamydomonas* sp. from the KOPRI culture collection of polar micro-organisms. Amino acid sequence analysis indicated the presence of three conserved histidine-rich segments as unique characteristics of omega-6 fatty acid desaturases, and three transmembrane regions transported to plastidic membranes by chloroplast transit peptides in the N-terminal region. The AChFAD6 desaturase activity was examined by expressing wild-type and V254A mutant (Mut-AChFAD6) heterologous recombinant proteins. Quantitative gas chromatography indicated that the concentration of linoleic acids in AChFAD6-transformed cells increased more than 3-fold [$6.73 \pm 0.13 \text{ mg g}^{-1}$ dry cell weight (DCW)] compared with cells transformed with vector alone. In contrast, transformation with Mut-AChFAD6 increased the concentration of oleic acid to $9.23 \pm 0.18 \text{ mg g}^{-1}$ DCW, indicating a change in enzymatic activity to mimic that of stearoyl-CoA desaturase. These results demonstrate that AChFAD6 of Arctic *Chlamydomonas* sp. increases membrane fluidity by enhancing denaturation of C18 fatty acids and facilitates production of large quantities of linoleic fatty acids in prokaryotic expression systems.

KEYWORDS

Arctic green microalga; *Chlamydomonas* sp.; fatty acid methyl ester; linoleic acid methyl ester; oleic acid methyl ester; psychrophilic

Introduction

The survival of cold-adapted micro-organisms, including Arctic green microalgae, is facilitated by unique characteristics of their proteins and membranes and their genetic responses to thermal changes.^[1] Many studies have focused on the activities of extracellular enzymes under cold conditions.^[2,3] Additionally, many species produce and maintain adequate concentrations of sugars and polyols that act as cryoprotectants, which lower the freezing point.^[4–8] The cellular membranes of psychrophilic micro-organisms comprise specific fatty acid components that maintain fluidity to transport substrates and avoid physical damage at low temperatures.^[9,10] Planktonic micro-organisms in a semisolid matrix undergo a phase shift from water to a semi or completely enclosed matrix.^[11] The desaturation of fatty acids with an appropriate number of bonds in the cis configuration can reduce the transition temperature from the solid to liquid crystalline phases by conferring sufficient membrane fluidity to microalgae living in the Arctic region.^[9]

Fatty acid desaturases (FADs) convert saturated fatty acids (SFAs) into mono and polyunsaturated fatty acids (MUFAs and PUFAs, respectively) by catalyzing desaturation reactions.^[9] Among the three types of FADs, acyl-ACP, and acyl-lipid desaturases catalyze desaturation of fatty acids in

plant cells.^[9,12,13] Transcription of the genes encoding acyl-lipid desaturases in *Synechocystis* was upregulated at low temperatures.^[14,15] Therefore, it was suggested that PUFA accumulation at low temperatures was due to upregulation of FAD expression.^[9] The omega-6 FAD (delta-12 FAD) catalyzes the introduction of a double bond at the delta-12 position of oleic fatty acid (C18:1 cis-9) to synthesize linoleic fatty acid (C18:2 cis,cis-9,12).^[16–18] Omega-6 FADs are categorized as FAD2 or FAD6 according to their localization within the endoplasmic reticulum and plastidial membranes, respectively.^[13,17,19] FAD6 may catalyze desaturation reactions to generate linoleic fatty acids in the chloroplast and plastidial membranes of Arctic *Chlamydomonas* spp. A recent transcriptomic analysis of an Arctic *Chlamydomonas* sp. (ArF0006) in the KOPRI culture collection of polar micro-organisms (KCCPM) was performed by pyrosequencing.^[20] The data revealed partial sequences of genes encoding putative desaturases and antifreeze proteins (AFPs).^[20]

In the present study, we performed rapid amplification of cDNA ends (RACE)-polymerase chain reaction (PCR) based on partial desaturase sequences and obtained a full-length cDNA of one ArF0006 FAD (AChFAD6). The deduced AChFAD6 was compared with FADs from various other organisms and its structural characteristics and cellular

CONTACT Sanghee Kim  sangheekim@kopri.re.kr  Division of Polar Life Sciences, Korea Polar Research Institute, Korea Institute of Ocean Science and Technology, Incheon 21990, Republic of Korea.

Color versions of one or more of the figures in the article can be found online at www.tandfonline.com/lpbb.

*Woongsic Jung and Eun Jae Kim were contributed equally to this work.

 Supplemental data for this article can be accessed on the publisher's website at <http://dx.doi.org/10.1080/10826068.2016.1188311>.

localization analyzed. Moreover, the activities of recombinant AChFAD6 and mutant AChFAD6 (Mut-AChFAD6) proteins were investigated by quantitative fatty acid methyl ester profiling.

Materials and methods

Isolation and culture of an Arctic *Chlamydomonas* sp

ArF0006, an Arctic *Chlamydomonas* sp., was isolated from ice-covered freshwater near the Dasan Station located in Ny-Ålesund, Spitsbergen, Norway (78°55'N, 11°56'E). Single cells of ArF0006 were maintained in the KCCPM. ArF0006 strains were grown in Tris-acetate phosphate medium under 25 $\mu\text{mol photon m}^{-2} \text{s}^{-1}$ (16:8-hr light/dark cycle) at 4°C. ArF0006 was identified as a *Chlamydomonas* sp. by morphological observation and molecular phylogeny in a previous study.^[20]

Isolation of an orf and analysis of the deduced omega-6 FAD amino acid sequence

ArF0006 cells were harvested by centrifugation at 5,000g for 10 min at 4°C. Total RNA was extracted using the RNeasy Plant Mini Kit (Qiagen, USA). Full-length cDNA was generated from total RNA using the 5'/3' RACE Kit, 2nd Generation (Roche, Germany). More than two forward and reverse primers based on the omega-6 FAD contig (ID, contig00093) nucleotide sequence were designed to determine whether the putative omega-6 FAD gene was present in ArF0006 cDNA (Table 1, Supplemental Table of Kim et al.^[20]). Gene-specific primers for amplification of the omega-6 FAD of ArF0006 were designed next (Table 1). After PCR amplification of ArF0006 omega-6 FAD (*AChFAD6*), the amplified products were examined by electrophoresis on a 1% agarose gel and subjected to DNA sequencing (Macrogen, Korea). The *AChFAD6* sequences were identified by tBlastx search against the amino acid sequences in the NCBI database.^[21] The *AChFAD6* sequences were deduced using the translation algorithm in the ExpASY package.^[22] The deduced amino acid sequences were examined using the following software packages: (1) SignalP^[23] for identification of signal peptides; (2) TargetP,^[24] ChloroP,^[25] PCLR chloroplast localization prediction,^[26] and LocTree2^[27] for analysis of localization of *AChFAD6*; and (3) HMMTOP,^[28] TMpred,^[29] and DAS^[30]

for prediction of secondary structures and transmembrane regions.

Alignment and phylogenetic analysis of *AChFAD6* and *FADs* from other organisms

Amino acid sequences that showed high identity with *AChFAD6* were identified in the NCBI database by comparison using the BlastP algorithm (*Arabidopsis lyrata* subsp. *lyrata*, XP_002867319; *A. thaliana*, NP_194824; *Descurainia sophia*, ABI_73993; *Brassica napus*, AAT_65208; *Nicotiana tabacum*, AIA_22326; *Solanum acaule*, AGW_21688; *S. cardiophyllum*, AGW_21690; *S. commersonii*, AGW_21689; *Tarenaya hassleriana*, XP_010548500; *Jatropha curcas*, ABU_96742; *Carthamus tinctorius*, AEK_06379; *Olea europaea*, AAW_63039; *Gossypium arboreum*, KHG_05619; *Theobroma cacao*, XP_007011948; *Portulaca oleracea*, ACB_14275; *Morus notabilis*, XP_010086850; *Arachis hypogaea*, ACZ_06070; *Medicago truncatula*, XP_003610331 and KEH_38076; *Glycine max*, NP_001238236; *Oryza sativa* var. *Japonica*, BAD_09897; *Ginkgo biloba*, AEJ_87848; *Physcomitrella patens*, XP_001778886; *Mesostigma viride*, ABD_58898; *Chlorella vulgaris* NJ-7, ADB03432; *Ch. vulgaris*, ACN59567; *Ch. variabilis*, XP005843960; *Coccomyxa subellipsoidea*, XP_005648776; *Auxenochlorella protothecoides*, XP_011397648; *Monoraphidium neglectum*, KIY_93798; *Chlamydomonas reinhardtii*, XP_001693068; *Chlamydomonas* sp. W80, BAA_83822; *Chlamydomonas* sp. ICE_L, AEK76074) (Figure 1). The selected amino acid sequences were aligned using the ClustalW algorithm.^[31] Phylogenetic analysis was performed by the distance method using 5,000 bootstrap repetitions. The unweighted pair group with arithmetic mean method was used to construct phylogenetic trees using the MEGA6 software.^[32]

The amino acid sequences of *AChFAD6* were aligned with those from green microalgae using the ClustalW algorithm^[31] in the BioEdit software.^[33] For alignment of amino acid sequences and analysis of conserved regions of *AChFAD6*, *Chlorella vulgaris* NJ-7 (Chlo_vul_01, ADB03432), *Chlorella vulgaris* (Chlo_vul_02, ACN59567), *Chlorella variabilis* (Chlo_var, XP005843960), *Chlamydomonas reinhardtii* (Chla_rei, XP001693068), and *Chlamydomonas* sp. ICE_L (Chla_sp, AEK_76074) were used (Figure 2).

Expression of *AChFAD6* in *E. coli*

To investigate *AChFAD6* activity, an expression construct was prepared using the pET32a (+) expression vector. The *AChFAD6* gene was amplified using gene-specific primers containing the restriction site sequences for the *Bam*HI and *Xho*I restriction enzymes (Table 1). Moreover, an *AChFAD6* mutant (V254A, Mut-AChFAD6) was produced by site-directed mutagenesis to assess the functional changes caused by replacement of amino acids in the third membrane-spanning region (Table 1). Purified *AChFAD6* PCR products and the pET32a (+) expression vector were digested with *Bam*HI and *Xho*I, and the digested products were purified and ligated using T4 DNA ligase (Elpisbio, Korea). Ligates were transformed into DH5 α *E. coli* competent cells

Table 1. Primers used in this study.

Name of primers	Sequences of primers (5'→3')
5'/3' RACE primers	
contig00093 5' RACE R2	CCAGGGGTCAAAGGGGTAGATG
contig00093 5' RACE R3	GATGGAGATGAGGAAGACGGAG
contig00093 3' RACE F2	GGCTACCACTTCTGGATGAGCA
contig00093 3' RACE F3	ATGTCCAAGATCCCGTGGTACAAC
contig00093 3' RACE F4	CTGCCAACAAACATGTAAAGGGC
Gene-specific primers	
<i>AChFAD6</i> _For	GCGG GAATCC ATGCAGGCAACAGCGTGTGC
<i>AChFAD6</i> _Rev	GCGG <u>CTCGAG</u> TTACATGTTGTTGGGCAGCA
Primers for site-directed mutagenesis	
V254-Sense	GAGCAGCAGAAGCCGCGCGCTGTGCA GCCTGGCAGCC
V254-Antisense	GGCTGCCAGGCTGACAAGCGCGCGCGG CTTCTGCTGCTC

(Young-In Frontier, Korea) and secondary antimouse IgG-horseradish peroxidase (Young-In Frontier, Korea) antibodies were used for Western blotting. Protein bands corresponding to AChFAD6s were detected using a colorimetric Western blot system (Opti-4CN Substrate Kit, Bio-Rad, USA).

Fatty acid composition of *E. coli* cells expressing AChFAD6

The fatty acid composition of cells harboring AChFAD6 and Mut-AChFAD6 was investigated by fatty acid methyl ester (FAME) analysis using a gas chromatograph (YL-6100GC, Korea) equipped with a flame ionization detector and a capillary column (Agilent, USA). Total lipids were extracted from 20 mg of freeze-dried samples as described previously.^[34] The fatty acid components in the organic phases were analyzed. FAME analysis was performed as follows: (1) 3 ml min⁻¹ in constant flow mode, (2) incubation at 100°C for 5 min followed by a temperature increase to 240°C (4°C min⁻¹), then a hold for 20 min, and (3) 250°C detector temperature. Chromatographic peaks of FAME components were assigned and quantified using the Supelco 37 Component FAME Mix as a standard (Sigma, USA). Total fatty acid contents were assessed based on the internal standard (1 mg C16:0 in hexane) together with the gas chromatographic peaks. Production yields are presented as milligrams FAMES per gram dry weight of *E. coli* cells. The gas chromatography analysis was performed three times independently.

Results

Isolation and characterization of AChFAD6

The ORF of the ArF0006 FAD gene (*AChFAD6*) was amplified and verified by 5'/3' RACE PCR from ArF0006 cDNA. The *AChFAD6* nucleotide sequence detected was 1,274 bp in length, including start and stop codons. The deduced amino acid sequence of AChFAD6 comprised 424 amino acids with a molecular weight of 48.2 kDa. Comparison of the nucleotide and amino acid sequences using the BLAST algorithm in NCBI resulted in categorization of AChFAD6 according to the delta-12 and omega-6 FADs.

Sequence alignment and phylogenetic analysis of AChFAD6

The phylogenetic relationships of AChFAD6 with other proteins were analyzed by comparison of their amino acid sequences. AChFAD6 showed high sequence identity to FADs of the following green microalgae strains: *Chlorella* sp. (GenBank ID, ACN59567; 94% sequence identity), *Chlorella* sp. NJ-7 (GenBank ID, ADB03432; 94% sequence identity), *Chlorella variabilis* (GenBank ID, XP_005843960; 81% sequence identity), *Chlamydomonas* sp. W80 (GenBank ID, BAA83822; 66% sequence identity), and *Chlamydomonas reinhardtii* (GenBank ID, XP_001693068; 64% sequence identity). Multiple alignment and phylogenetic analyses using the ClustalW algorithm^[31] and MEGA6^[33] demonstrated that omega-6 FADs from higher plants and green microalgae existed separately, and AChFAD6 was closely associated with

the clade of green microalgal omega-6 FADs (Figure 1). This result strongly suggested AChFAD6 to be a green microalgal FAD that converts MUFAs into PUFAs.

In silico characterization of AChFAD6 amino acid sequences

Three conserved histidine-rich domains (amino acids 148–152, 184–188, and 346–350) were detected in the AChFAD6 sequence; these are important for fatty acid desaturation (Figure 2).^[9,35,36] The primary and secondary structures of AChFAD6 were analyzed using computational software. First, AChFAD6 is likely intracellular due to the absence of signal peptides, as determined using the SignalP software (Figure S1).^[23] AChFAD6 was found to be located in chloroplast membranes by TargetP^[24] and ChloroP software.^[25] ChloroP provided information regarding the length of presumed chloroplast transit peptides (cTPs). The PCLR chloroplast localization prediction software^[26] robustly supported the chloroplast localization of AChFAD6, with a high value of 0.861 (threshold for predicted chloroplast targeting, 0.42). In addition, the localization of AChFAD6 was predicted using the LocTree2 software (Figure S2).^[27] The secondary structure and transmembrane regions of AChFAD6 were next investigated based on the amino acid sequence. The entire sequence of AChFAD6 comprised α -helices and β -strands (Figure 3). Three chloroplast membrane-spanning regions were identified using the TMpred^[29] and DAS^[30] software packages (Figures 3 and 4). These membrane-spanning regions comprised α -helices, and histidine-rich motifs were located within or near the α -helix structures. Moreover, mapping of disulfide bonds of eight cysteine residues in AChFAD6 sequences using the DIpro software^[37] in the SCRATCH protein predictor package resulted in prediction of three disulfide bonds (6Cys–17Cys, C124–C150, and C330–C340) (Figure 3). The 50Cys and 392Cys residues were found to retain free thiol functional groups.

Recombinant expression and detection of AChFAD6s in *E. coli*

The enzymatic activity of recombinant AChFAD6s expressed in *E. coli* was investigated. One mutagenic AChFAD6 (V254A, Mut-AChFAD6) was generated by site-directed mutagenesis to monitor the effect of substitution of an amino acid in the third membrane-spanning region. The pET32a (+) expression vector was used to ensure correct folding of AChFAD6s in *E. coli*. Recombinant AChFAD6 and Mut-AChFAD6 were expected to be of 68.2 kDa. As no SDS-PAGE band was observed, Western blot analysis was performed to detect expression at levels as low as nanograms per microliter (Figure 5a). Colorimetric immunoblot analysis indicated successful expression of both AChFAD6s at the predicted molecular weights (Figure 5b).

Fatty acid composition of *E. coli* cells harboring AChFAD6s

The fatty acid composition of *E. coli* harboring AChFAD6 and Mut-AChFAD6 was investigated by gas chromatography

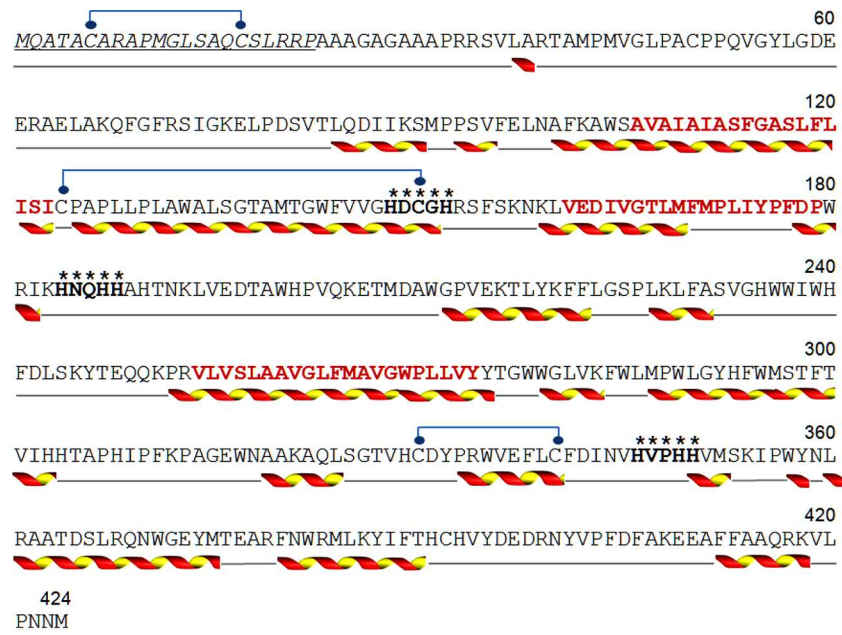


Figure 3. Amino acid sequence and secondary structure analyses of AChFAD6. Italic and underlined amino acid sequences indicate chloroplast transit peptides. Bold and red amino acid sequences represent chloroplast and plastid transmembrane regions. Cysteine residues and disulfide linkages are indicated by blue dots and blue lines, respectively. The histidine-rich motifs are indicated by upper asterisks and bold characters. α -helices and β -strands are indicated by gray lines and yellow-red ribbons, respectively.

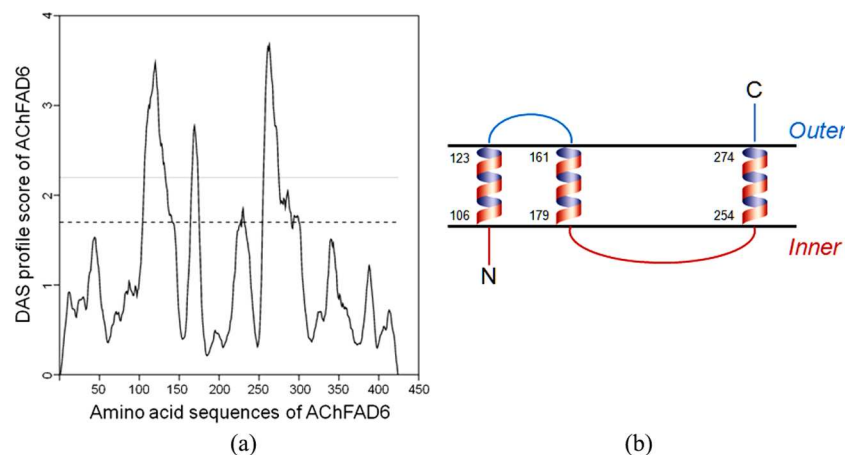


Figure 4. Prediction of transmembrane fragments of AChFAD6. (a) Dense alignment surface profile of AChFAD6. Strict cutoffs are shown as lines and (b) AChFAD6 transmembrane fragment pattern. Numbers to the left of the helices indicate the locations of amino acids.

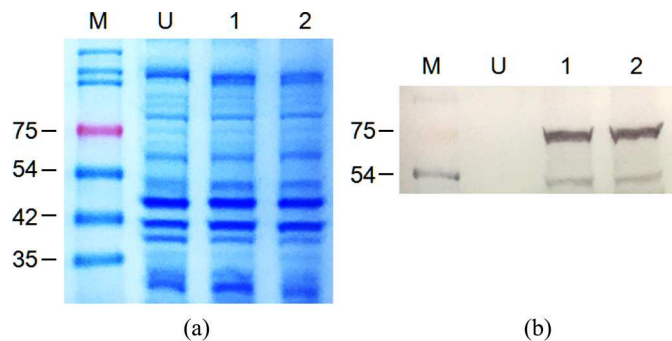


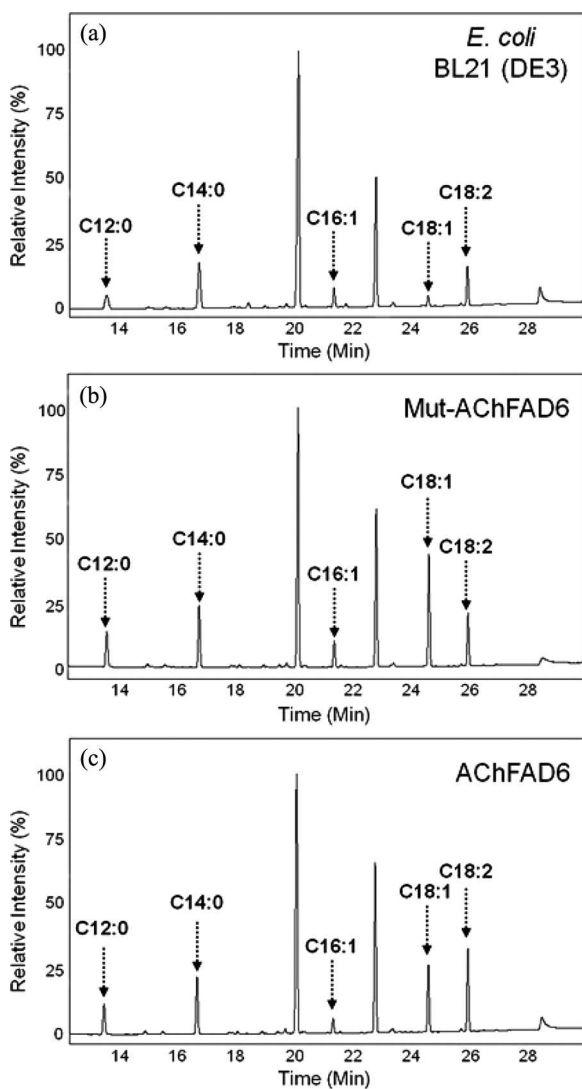
Figure 5. Heterologous expression of recombinant AChFAD6s in *E. coli* and detection by immunoblotting. (a) Coomassie blue staining and (b) Western blot analysis. M, protein size marker; U, *E. coli* cells harboring the pET32a (+) vector (negative control); 1, *E. coli* cells harboring AChFAD6; 2, *E. coli* cells harboring Mut-AChFAD6.

FAME analysis. Total fatty acids were extracted from 20 mg dry weight of *E. coli* expressing pET32a (+) (negative control), AChFAD6, and Mut-AChFAD6. Total fatty acid levels were 38.07 ± 0.97 , 63.66 ± 1.27 , and 64.71 ± 0.97 mg g⁻¹ DCW for the negative control, AChFAD6, and Mut-AChFAD6, respectively (Table 2). Oleic (C18:1, *n*-9) and linoleic (C18:2, *n*-9,12) acid levels were elevated in cells expressing AChFAD6 (Figure 6b). In cells expressing Mut-AChFAD6, the oleic acid concentration was significantly higher (Figure 6c). Oleic and linoleic acid levels in cells expressing AChFAD6 were 7- and 2-folds higher, respectively (5.45 ± 0.16 and 6.73 ± 0.13 mg g⁻¹ DCW, respectively), compared with the negative control (Table 2). The oleic acid concentration significantly increased by ~10-fold (9.23 ± 0.18 mg g⁻¹) in cells harboring Mut-AChFAD6 (Table 2). Therefore, AChFAD6 and

Table 2. Dominant contents of fatty acid methyl esters (FAMES) in expressed *E. coli* cells modified by induction of AChFAD6 and mutant AChFAD6 (Mut-AChFAD6).

Micro-organisms analyzed	pET32a (+) (negative control)	Induced cells by AChFAD6	Induced cells by Mut-AChFAD6	<i>C. reinhardtii</i> CC-125
<i>Escherichia coli</i>				
C12:0 [mg g ⁻¹ (%)	1.54 ± 0.05 (4.06 ± 0.24%)	2.99 ± 0.17 (5.32 ± 0.97%)	3.48 ± 0.17 (5.39 ± 0.35%)	N/D
C14:0 [mg g ⁻¹ (%)	3.85 ± 0.15 (10.13 ± 0.65%)	5.02 ± 0.25 (8.93 ± 1.58%)	5.38 ± 0.21 (8.32 ± 0.45%)	N/D
C16:1 [mg g ⁻¹ (%)	1.11 ± 0.06 (2.92 ± 0.23%)	1.26 ± 0.05 (2.24 ± 0.38%)	2.23 ± 0.07 (3.45 ± 0.16%)	1.00 ± 0.02 (0.77 ± 0.03%)
C18:1 [mg g ⁻¹ (%)	0.56 ± 0.05 (1.48 ± 0.17%)	5.45 ± 0.16 (9.67 ± 1.52%)	9.23 ± 0.18 (14.27 ± 0.49%)	1.40 ± 0.04 (1.08 ± 0.05%)
C18:2 [mg g ⁻¹ (%)	2.06 ± 0.12 (5.43 ± 0.45%)	6.73 ± 0.13 (11.92 ± 1.76%)	4.24 ± 0.13 (6.56 ± 0.30%)	N/D
Total fatty acids (mg g ⁻¹)	38.07 ± 0.97	63.66 ± 1.27	64.71 ± 0.97	130.00 ± 1.56

N/D, not detected.

**Figure 6.** Gas chromatography peak profiles of total fatty acids. (a) *E. coli* cells harboring pET32a (+) (negative control) and (b) *E. coli* cells harboring AChFAD6, and (c) *E. coli* cells harboring Mut-AChFAD6.

Mut-AChFAD6 derived by single substitution with nonpolar amino acid residues in the membrane-spanning region might catalyze introduction of double bonds at different positions in SFAs.

Discussion

The genus *Chlamydomonas* is highly adaptable. Photosynthetic micro-organisms living in polar regions play important

roles in aquatic ecosystems as primary producers. ArF0006 in the KCCPM provides a good model for the investigation of genes related to environmental stress and cold adaptation, such as those encoding FADs and AFPs.^[20] Among the genes identified by transcriptomic analysis of ArF0006, the FAD gene was investigated. The full-length cDNA of ArF0006 FAD (AChFAD6) was determined to comprise 1,274 bp encoding 424 amino acids. The amino acid sequence of AChFAD6 showed a sequence identity of up to 94% with FADs from two strains of the genus *Chlorella*. Phylogenetic analysis of the amino acid sequences of AChFAD6s and FADs from a wide range of organisms, including higher plants, indicated AChFAD6 to be a typical FAD of green microalgae, completely separate from the FADs of higher plants (Figure 1). Therefore, these two types of organisms possess FADs with different amino acid sequences and thus likely evolved separately.

Omega-6 fatty acid desaturase gene contains three histidine-rich motifs (HDCGH, HNQH, and HVPHH) based on alignment with the sequences of five FADs of green microalgae. These conserved histidine motifs are typical features of FADs and catalyze the binding of ferric ions.^[9,10,38,39] These amino acid sequence characteristics have been reported in delta-12 and omega-3 FADs from Antarctic *Chlorella* sp. and *Chlamydomonas* sp.^[17,40] Currently, the structure and substrate specificity of acyl-CoA delta-9 desaturases from the marine copepod *Calanus hyperboreus* were reported.^[10] The second membrane-spanning fragment is crucial for the desaturase activity of *C. hyperboreus* delta-9 desaturases, and tyrosine in this integrated region is a key residue for determining the length of the fatty acid chains of the substrates.^[10] The primary and secondary structures of AChFAD6 sequences were analyzed in detail. Twenty-two amino acids in the N-terminal region were predicted in silico to be cTPs.^[24–27]

The following three criteria for the determination of stromal-targeting transit peptides have been reported:^[12,41] (1) an uncharged N-terminal domain beginning with Met-Ala and terminating with a Gly or Pro residue; (2) the absence of acidic residues and enrichment of Ser or Thr in the central domain; and (3) enrichment of Arg residues in the C-terminal domain.^[41] First, the amino acid sequence of the N-terminal region of AChFAD6 was found to begin with Met-Gln-Ala and end with a Pro residue at position 22. The uncharged amino acids Cys, Pro, Gln, and Thr were distributed among the first 10 amino acid residues. Second, three Ser/Thr residues were detected, but no acidic residues were identified. Finally, two continuous Arg residues were present in the C-terminal

domain. Therefore, AChFAD6 would be categorized as a FAD6 isoform localized in the chloroplast membrane and the stromal space within the chloroplast.^[13,17,19] The secondary structure of AChFAD6 includes three α -helix structures within the chloroplast membrane. The first and third conserved histidine-rich motifs were exposed to the cytosolic compartment, and the second was located inside the chloroplast. Similar to *C. hyperboreus* delta-9 desaturases, a tyrosine residue (175Y) was present in the second transmembrane region. Among the three disulfide bonds predicted by Dipro,^[37] the second disulfide bridge (124C–150C) is responsible for interactions with ligands such as ferric irons. The cysteine residue at position 124 is the first residue exposed to the cytosol, and 150Cys is positioned in the center of the first conserved histidine-rich motif. The peptide region including 124Cys and 150Cys is contained within the catalytic center of the C-terminal region and interacts with ligand ions.^[9,10] These findings suggest that the disulfide cross-link in the catalytic domain exposed to the cytosolic compartment contributes to maintenance of the catalytic structure in which the histidine residues bind to ligands.^[14,18]

To evaluate the desaturase activity of AChFAD6s, recombinant proteins were produced using a prokaryotic expression system. In addition, a single nucleotide substitution of valine for alanine was generated by site-directed mutagenesis. The 254 Val is the starting residue and a component of the α -helix in the third integral membrane region. Therefore, mutation from Val to Ala, a small nonpolar amino acid, might alter the activity of Mut-AChFAD6. Expression of *AChFAD6* and *Mut-AChFAD6* in *E. coli* was induced by 1 mM IPTG and detected as clear bands of the expected molecular weights. Omega-6 FADs catalyze the conversion of monoenoic into dienoic fatty acids, which play key roles in maintenance of membrane fluidity at low temperatures.^[9,16,17] Cells harboring AChFAD6 and Mut-AChFAD6 showed different patterns of oleic (C18:1, *n*-9) and linoleic (C18:2, *n*-9,12) acids (Figure 6 and Table 2). The linoleic acid concentration was higher than that of oleic acid in cells harboring AChFAD6. The linoleic acid composition ($11.92 \pm 1.76\%$) was 2-fold higher than that of the negative control ($5.43 \pm 0.45\%$). Moreover, the ratio of linoleic acid to total fatty acids was higher than that of oleic acid ($9.67 \pm 1.52\%$). These results suggest AChFAD6 to be a typical omega-FAD catalyzing the desaturation of MUFAs into PUFAs. However, the fatty acid profile of *E. coli* expressing Mut-AChFAD6 differed significantly from that of AChFAD6. Surprisingly, a single point mutation resulting in a single amino acid substitution modified the activity of the wild-type enzyme. First, Mut-AChFAD6-expressing cells showed a high oleic acid concentration, in contrast to AChFAD6-expressing cells (Figure 6c). Similarly, oleic and linoleic acid concentrations differed between cells harboring AChFAD6 and Mut-AChFAD6 (Table 2). The oleic acid concentration ($14.27 \pm 0.49\%$) was ~10-fold higher than that of the negative control ($1.48 \pm 0.17\%$). Moreover, cells harboring Mut-AChFAD6 exhibited a ~4.60% higher C18:1 fatty acid concentration ($14.27 \pm 0.49\%$) than that of cells bearing AChFAD6 ($9.67 \pm 1.52\%$). In contrast, Mut-AChFAD6 expression induced a linoleic acid concentration of $6.56 \pm 0.30\%$, which was lower than that by AChFAD6 expression. Mut-AChFAD6 showed

enzymatic activity similar to that of stearoyl-CoA desaturase (SCD); i.e., conversion of SFAs into MUFAs.^[9,10,39] Valine and alanine are hydrophobic due to their aliphatic side chains. However, these two amino acids have different molecular weights (99.1 and 71.1 Da for valine and alanine, respectively) and hydrophathy scales (4.2 and 1.8 for valine and alanine, respectively). The first amino acid and its neighbors in the third membrane-spanning domain may thus be the targets for genetic modification to improve enzymatic activities and to increase the PUFA yield for industrial applications.

In conclusion, we performed genetic, structural, and functional analyses of a chloroplast-targeted omega-6 FAD from Arctic *Chlamydomonas* sp. AChFAD6. AChFAD6 was grouped with FADs and was found to contain cTPs, three membrane-spanning regions and three conserved histidine-rich motifs, which are typical features of chloroplast-specific FADs from green microalgae. The structure and enzymatic activity of AChFAD6 were similar to those of the chloroplast-targeting omega-6 FADs of psychrophilic microorganisms. An amino acid substitution (V254A) in the third transmembrane domain resulted in a change from FAD to SCD activity. Mut-AChFAD6 should be further investigated by site-directed mutagenesis and subjected to structural analysis by X-ray crystallography.

Conclusion

The gene and the deduced amino acid sequences of omega-6 fatty acid desaturase were isolated to reveal the survival of Arctic *Chlamydomonas* sp. in cold environment and to identify enzymatic activity in the heterologous system. Arctic *Chlamydomonas* sp. omega-6 fatty acid desaturase with 48.2 kDa showed enzymatic activity enhancing the concentration of linoleic fatty acid in the *E. coli* expression system. In addition, site-directed mutant, V254A, showed high SCD activity, that was different activity to wild type. From the result, the first amino acid in third membrane-spanning region is crucial to maintain omega-6 fatty acid desaturase activity. Therefore, genetic modification on the membrane-spanning regions of FADs might increase the yield of target fatty acids and modulate enzymatic activities for industrial application.

Acknowledgment

This work was supported by the basic research program (PE16020) of the Korea Polar Research Institute (KOPRI), by a grant (PN15070) of Korea Institute of Planning and Evaluation for Technology in Food, Agriculture, Forestry and Fisheries (iPET) and by KOPRI Project (PM15040) of Ministry of Oceans and Fisheries (MOF).

References

- [1] Deming, J.W. Psychrophiles and Polar Regions. *Curr. Opin. Microbiol.* **2002**, *23*, 301–309.
- [2] Huston, A.L.; Krieger-Brockett, B.B.; Deming, J.W. Remarkably Low Temperature Optima for Extracellular Enzyme Activity from Arctic Bacteria and Sea Ice. *Environ. Microbiol.* **2000**, *2*, 383–388.
- [3] Deming, J.W.; Baross, J.A. *Enzymes in the Environment*. Marcel Dekker, New York, 2001.

- [4] Block, W.; Burns, A.J.; Richard, K.J. An Insect Introduction to the Maritime Antarctic. *Biol. J. Linn. Soc.* **1984**, *23*, 33–39.
- [5] Cannon, R.J.C.; Block, W. Cold Tolerance of Microarthropods. *Biol. Rev. Camb. Philos. Soc.* **1988**, *63*, 23–77.
- [6] Block, W.; Duman, J.G. The Presence of Thermal Hysteresis Producing Antifreeze Proteins in the Antarctic Mite, *Alaskozetes Antarcticus*. *J. Exp. Zool.* **1989**, *250*, 229–231.
- [7] Convey, P. Overwintering Strategies of Terrestrial Invertebrates in Antarctica—the Significance of Flexibility in Extremely Seasonal Environments. *Eur. J. Entomol.* **1996**, *93*, 489–505.
- [8] Worland, M.R.; Block, W.; Grubor-Lajsic, G. Survival of *Heleomyza borealis* (Diptera, Helemyzidae) Larvae Down to -60°C . *Physiol. Entomol.* **2000**, *25*, 1–5.
- [9] Los, D.A.; Murata, N. Structure and Expression of Fatty acid Desaturases. *Biochim. Biophys. Acta* **1998**, *1394*, 3–15.
- [10] Meesapyodsuk, D.; Qiu, X. Structure Determinants for the Substrate Specificity of Acyl-CoA $\Delta 9$ Desaturases from a Marine Copepod. *ACS Chem. Biol.* **2014**, *9*, 922–934.
- [11] Krembs, C.K.; Eicken, H.; Junge, K.; Deming, J.W. High Concentrations of Exopolymeric Substances in Arctic Winter Sea Ice: Implications for the Polar Ocean Carbon Cycle and Cryoprotection of Diatoms. *Deep-Sea Res. I* **2002**, *49*, 2163–2181.
- [12] Claros, M.G.; Brunak, S.; von Heijne, G. Prediction of N-terminal Protein Sorting Signals. *Curr. Opin. Struct. Biol.* **1997**, *7*, 394–398.
- [13] Shanklin, J.; Cahoon, E.B. Desaturation and Related Modifications of Fatty Acids. *Annu. Rev. Plant Physiol.* **1998**, *49*, 611–641.
- [14] Petersen, M.T.N.; Jonson, P.H.; Petersen, S.B. Amino Acid Neighbours and Detailed Conformational Analysis of Cysteines in Proteins. *Prot. Eng.* **1999**, *12*, 535–548.
- [15] Davies, P.L. Ice-binding Proteins: A Remarkable Diversity of Structures for Stopping and Starting Ice Growth. *Trends Biochem. Sci.* **2014**, *39*, 548–555.
- [16] Miyasaka, H.; Tanaka, S.; Kanaboshi, H. Cloning and Expression of a Gene Encoding a Putative Chloroplast Omega-6 Fatty Acid Desaturase of Marine *Chlamydomonas*. *Plant Biotechnol.* **2000**, *17*, 167–171.
- [17] Lu, Y.; Chi, X.; Li, Z.; Yang, Q.; Li, F.; Liu, S.; Gan, Q.; Qin, S. Isolation and Characterization of a Stress-dependent Plastidial Delta12 Fatty Acid Desaturase from the Antarctic Microalga *Chlorella Vulgaris* NJ-7. *Lipids* **2010**, *45*, 179–187.
- [18] Turk, V.; Stoka, V.; Vasiljeva, O.; Renko, M.; Sun, T.; Turk, B.; Turk, D. Cysteine Cathepsins: from Structure, Function and Regulation to New Frontiers. *Biochim. Biophys. Acta* **2012**, *1824*, 68–88.
- [19] Sakuradani, E.; Kobayashi, M.; Ashikari, T.; Shimizu, S. Identification of Delta 12-fatty Acid Desaturase from Arachidonic Acid-producing *Mortierella* Fungus by Heterologous Expression in the Yeast *Saccharomyces Cerevisiae* and the Fungus *Aspergillus Oryzae*. *Eur. J. Biochem.* **1999**, *261*, 812–820.
- [20] Kim, S.; Kim, M.J.; Jung, M.G.; Lee, S.; Baek, Y.S.; Kang, S.H.; Choi, H.G. De Novo Transcriptome Analysis of an Arctic Microalga, *Chlamydomonas* sp. *Genes Genom.* **2013**, *35*, 215–223.
- [21] Altschul, S.F.; Gish, W.; Miller, W.; Myers, E.W.; Lipman, D.J. Basic Local Alignment Search Tool. *J. Mol. Biol.* **1990**, *215*, 403–410.
- [22] Artimo, P.; Jonnalagedda, M.; Arnold, K.; Baratin, D.; Csardi, G.; de Castro, E.; Duvaud, S.; Flegel, V.; Fortier, A.; Gasteiger, E.; Grosdidier, A.; Hernandez, C.; Ioannidis, V.; Kuznetsov, D.; Liechti, R.; Moretti, S.; Mostaguir, K.; Redaschi, N.; Rossier, G.; Xenarios, I.; Stockinger, H. ExPASy: SIB Bioinformatics Resource Portal. *Nucleic Acids Res.* **2012**, *40*, W597–W603.
- [23] Petersen, T.N.; Brunak, S.; von Heijne, G.; Nielsen, H. SignalP 4.0: Discriminating Signal Peptides from Transmembrane Regions. *Nat. Methods* **2011**, *8*, 785–786.
- [24] Emanuelsson, O.; Brunak, S.; von Heijne, G.; Nielsen, H. Locating Proteins in the Cell Using TargetP, SignalP and Related Tools. *Nat. Protoc.* **2007**, *2*, 953–971.
- [25] Emanuelsson, O.; Nielsen, H.; von Heijne, G. ChloroP, a Neural Network-based Method for Predicting Chloroplast Transit Peptides and their Cleavage Sites. *Protein Sci.* **1999**, *8*, 978–984.
- [26] Schein, A.I.; Kissinger, J.C.; Ungar, L.H. Chloroplast Transit Peptide Prediction: A Peek Inside the Black Box. *Nucleic Acids Res.* **2001**, *29*, e82.
- [27] Goldberg, T.; Hamp, T.; Rost, B. LocTree2 Predicts Localization for all Domains of Life. *Bioinformatics* **2012**, *28*, i458–i465.
- [28] Tusnady, G.E.; Simon, I. The HMMTOP Transmembrane Topology Prediction Server. *Bioinformatics* **2001**, *17*, 849–850.
- [29] Hofmann, K.; Stoffel, W. TMbase - A Database of Membrane Spanning Proteins Segments. *Biol. Chem. Hoppe-Seyler* **1993**, *374*, 166.
- [30] Cserzo, M.; Wallin, E.; Simon, I.; von Heijne, G.; Elofsson, A. Prediction of Transmembrane Alpha-helices in Prokaryotic Membrane Proteins: The Dense Alignment Surface Method. *Prot. Eng.* **1997**, *10*, 673–676.
- [31] Thompson, J.D.; Higgins, D.G.; Gibson, T.J. CLUSTAL W: Improving the Sensitivity of Progressive Multiple Sequence Alignment Through Sequence Weighting, Position Specific Gap Penalties and Weight Matrix Choice. *Nucleic Acids Res.* **1994**, *11*, 4673–4680.
- [32] Tamura, K.; Stecher, G.; Peterson, D.; Filipowski, A.; Kumar, S. MEGA6: Molecular Evolutionary Genetics Analysis Version 6.0. *Mol. Biol. Evol.* **2013**, *30*, 2725–2729.
- [33] Hall, T.A. BioEdit: A User-friendly Biological Sequence Alignment Editor and Analysis Program for Windows 95/98/NT. *Nucl. Acids Symp. Ser.* **1999**, *41*, 95–98.
- [34] Sasser, M. *Identification of Bacteria by Gas Chromatography of Cellular Fatty Acids*. Microbial ID Inc.: Newark, Del, 1990.
- [35] Thiede, M.A.; Ozols, J.; Strittmatter, P.J. Construction and Sequence of cDNA for Liver Stearoyl Coenzyme A Desaturase. *J. Biol. Chem.* **1986**, *261*, 13230–13235.
- [36] Falcone, D.L.; Gibson, S.; Lemieux, B.; Somerville, C. Identification of a Gene that Complements an *Arabidopsis* Mutant Deficient in Chloroplast Omega 6 Desaturase Activity. *Plant Physiol.* **1994**, *106*, 1453–1459.
- [37] Cheng, J.; Saigo, H.; Baldi, P. Large-scale Prediction of Disulphide Bridges Using Kernel Methods, Two-dimensional Recursive Neural Networks, and Weighted Graph Matching. *Proteins* **2006**, *62*, 617–629.
- [38] Alonso, D.L.; Garcia-Maroto, F.; Rodriguez-Ruiz, J.; Garrido, J.A.; Vilches, M.A. Evolution of the Membrane-bound Fatty Acid Desaturases. *Biochem. Syst. Ecol.* **2003**, *31*, 1111–1124.
- [39] Heinemann, F.S.; Ozols, J. Stearoyl-CoA Desaturase, a Short-lived Protein of Endoplasmic Reticulum with Multiple Control Mechanisms. *Prostag. Leukotr. Ess.* **2003**, *68*, 123–133.
- [40] Zhang, P.; Liu, S.; Cong, B.; Wu, G.; Liu, C.; Lin, X.; Shen, J.; Huang, X. A Novel Omega-3 Fatty Acid Desaturase Involved in Acclimation Processes of Polar Condition from Antarctic Ice Algae *Chlamydomonas* sp. ICE-L. *Mar. Biotechnol.* **2011**, *13*, 393–401.
- [41] Bruce, B.D. Chloroplast Transit Peptides: Structure, Function and Evolution. *Trends Cell. Biol.* **2000**, *10*, 440–447.